

# Wireless Temperature Sensors for Health Monitoring of Aerospace Thermal Protection Systems

Frank S. Milos and Joan B. Pallix  
NASA Ames Research Center, Moffett Field, CA 94035-1000

## ABSTRACT

Health diagnostics is an area where major improvements have been identified for potential implementation into the design of new reusable launch vehicles in order to reduce life-cycle costs, to increase safety margins, and to improve mission reliability. NASA Ames is leading the effort to advance inspection and health management technologies for thermal protection systems. This paper summarizes a joint project between NASA Ames and industry partners to develop "wireless" devices that can be embedded in the thermal protection system to monitor temperature or other quantities of interest. These devices are sensors integrated with radio-frequency identification microchips to enable non-contact communication of sensor data to an external reader that may be a hand-held scanner or a large portal through which the entire vehicle may be passed. Both passive and active (battery assisted) prototype devices have been developed. The passive device uses a thermal fuse to indicate the occurrence of excessive temperature. The active device uses a thermocouple to measure temperature history.

**Keywords:** damage detection, embedded sensor, nondestructive evaluation, RFID, thermal protection systems, wireless communication.

## INTRODUCTION

Commercialization of a competitive reusable launch vehicle (RLV) to replace the aging Space Shuttle fleet is a primary goal for both NASA and the US aerospace industry [1-2]. To expedite achievement of this goal, NASA is funding development of innovative technologies to lower cost and to increase safety and reliability for access to space. Vehicle ground operations for the thermal protection system (TPS) is one area where significant improvements are required. Current Space Shuttle procedures rely almost entirely on humans to perform a detailed close-range visual inspection of the entire exterior surface, identifying defects and dimensioning them as required for disposition (ignore, repair, replace) using measurement aids such as rulers, micrometers, and depth gauges [3]. This work is both time consuming and tedious. Compared with these current Shuttle procedures, ground operations for future RLVs need lower personnel costs as well as much faster turnaround time. Vehicle turnaround in days, rather than months, is the goal for the next-generation RLV. Therefore, TPS inspection and certification for flight must take hours, rather than weeks.

Non-destructive evaluation (NDE) technology is expected to make future TPS inspection activities more automated, more reliable, and quicker than human inspections. Figure 1 shows a futuristic concept of TPS inspection operations for a RLV [4]. A large portal is used to scan the entire vehicle, inspecting the exterior surface for damage and querying a suite of subsurface health sensors to confirm their operational status [5]. Alternative concepts to accomplish the same objective from a closer distance are: automated scanning heads that can sweep the surface of vehicle, or a set of small light-weight robots that can walk around the vehicle surface (possibly doing repairs as required). Robots would be useful for in-space inspection and repair of a vehicle docked at the International Space Station. In any case, the surface inspection probably will utilize a combination of a smart color vision system, a 3-D laser measurement tool, and pattern recognition software. The subsurface sensor data would be acquired using wireless communication from the individual sensors or from the vehicle. The scan results are compared with a historical database of internal sensor and surface data to assess the health and launch readiness of the vehicle. All anomalies are noted, and if none require immediate attention, the vehicle may proceed to launch. The same system can be used for post-flight inspection and download of flight sensor data.

NASA Ames has been identified as the lead center to develop TPS inspection and health management technologies. To this end, cooperative research is being carried out with various industry partners and other NASA centers to develop in parallel both optical surface inspection technology and subsurface sensor technology. In both cases, although the inspection system eventually will be fully automated, portable handheld inspection tools will be developed for near-term applications involving human inspectors. These handheld tools will be less costly for sensor system development and testing, and they can be used on the Shuttle to assist in meeting a goal to complete ground operations in 30 days. This paper summarizes recent development efforts for subsurface TPS health sensors [6-7]. The optical surface scanning system will be the subject of a different paper.

## **REQUIREMENTS DEFINITION**

Once the inspection portal concept (Figure 1) was identified as a long-term goal, a list of system requirements for remote automated inspection technology was developed cooperatively by TPS and sensors experts and operations personnel at Kennedy Space Center (KSC). The primary requirements are:

1. Must provide rapid inspection for fast vehicle turnaround.
2. Must carry out the inspection with high reliability and reproducibility.
3. Development and implementation costs must be reasonable.
4. Must be safe for humans and vehicles.
5. No excessive database or data processing requirements.
6. Should be applicable to all TPS to minimize the number of systems required.
7. Should be easily integrable into an overall integrated vehicle health management (IVHM) system.

Most of these requirements are straightforward and driven by NASA goals for cost, reliability, safety, and schedule. For TPS subsurface sensors, the following requirements were added:

8. Must be sufficiently small and lightweight.
9. Must not adversely impact the TPS thermal or mechanical performance.
10. Insertion must have minimal impact on TPS manufacturing costs.
11. Lifetime must exceed TPS lifetime, or design must allow easy replacement and maintenance.
12. Communications must be wireless.

The TPS presents special difficulties and requirements for instrumentation. The TPS consists of thousands of separate parts that are independently bonded to an underlying structure and independently replaceable in case of damage. To monitor the health of every significant part will require thousands of sensors (25,000 on a large vehicle is not unrealistic), however the sensors and the data acquisition system need to have minimal overall mass and volume impact on the vehicle. Therefore, the average mass per sensor should be only a fraction of a gram. Furthermore, the sensor data collection system cannot rely on wiring (metallic, fiber optic) between parts, because of the mass of extensive wiring and the difficulty in locating and repairing damaged wires. TPS components are designed to last from tens to hundreds of flights and (ideally) should not be replaced except as required owing to damage such as a debris impact hole. Subsurface instrumentation must have a longer lifetime than the TPS, because sensors will not be allowed to drive the TPS replacement schedule. Finally, the sensors also must survive adverse environmental conditions, most notably temperature extremes that can vary from sub-zero in space to over 1200°C at the surface during entry. Extremely low temperatures are possible at locations near cryogenic tanks.

## **TECHNICAL APPROACH**

In consideration of the formidable requirements for instrumentation, in particular the need to collect sensor data without use of extensive wiring, our initial concept is to forgo an onboard data acquisition system and instead rely on the external portal or portable reader to collect data directly from subsurface sensors. The sensors will be mutually independent. Each sensor is attached to a radio-frequency-tuned circuit containing a radio-frequency identification (RFID) microchip. Figure 2 shows a functional block diagram for the system, consisting of an external macro-reader and

any number of micro-devices [5]. The reader radiates sufficient radio-frequency power to energize the sensor circuit. An identification number is retrieved from the microchip's memory, and the ID number and sensor data are transponded back to the reader. The sensor data may be the current state of the sensor (e.g., are you still waterproofed?), a previously recorded sensor state (e.g., the maximum temperature measured during this mission), or a detailed profile of flight data. A microbattery optionally can be used to provide power for in-flight data acquisition and to assist on-ground data transmission.

One important question to answer is whether or not wireless communication at standard RF frequencies is effective through TPS materials. Tests using off-the-shelf technology showed that RF communication at 125 kHz and 13.56 MHz was feasible through various commonly-used, low-density TPS tiles and blankets. For example, using "rice-grain"-sized commercial RFID tags and a small reader (Figure 3), a read range of about 10 cm from the sensor was observed with variations of about 10% depending on the combinations of materials being tested. The read range needs to be increased significantly, because in some applications the TPS may be 10-cm thick, but there appears to be no fundamental problem using RF communications to and from subsurface sensors.

The other major communications issue is the speed with which sensors can be read. A "wing-shaped" demonstration article (Figure 4) was assembled with over one hundred RFID tags beneath a TPS blanket and tiles. The reader is an 18-cm square coil. The RFID microchips and reader utilize "anticollision" technology to enable communications with multiple tags of the same type. The demonstration shows that communication with all tags easily can be accomplished in less than one minute from a distance of over 30 cm. The implication for a RLV is that multiple readers or receiving stations may be needed to read tens of thousands of tagged sensors. If the overall power requirement, anticollision capability, or read range are a problem at the length scale of a large portal, the use of moving scan heads or robots that can get closer to the vehicle surface should mitigate these problems.

Faster communication or greater read distance may be possible using RFID components that operate at higher frequencies such as 900 MHz; however, these components require higher power and may be difficult to operate in a passive mode with a small microantenna. Determination of an optimal frequency for communication is an active area of research.

## **PROTOTYPE PASSIVE SENSOR**

A review of Shuttle inspection operations identified several potential applications of TPS health sensors such as monitoring internal temperatures, measuring the burnout depth of waterproofing agents, and detecting impact by micrometeorites or orbital debris. The detection of overheating at the bond-line between the TPS and the structure in inter-tile gaps received the highest priority from KSC operations personnel. Therefore, the initial focus of this work was to develop a tagged sensor suitable for detecting excessive temperatures in gaps and small enough to allow testing on the Space Shuttle.

Figure 5 provides a diagram of the Shuttle TPS geometry. The tile thickness varies from 2.6 to 10.2 cm, and inter-tile gaps nominally vary from 0.08 to 0.13 cm. On reentry from orbit, hot gas penetration into the gap can char the filler bar, RTV bond, and felt strain isolation pad (SIP). If this subsurface damage is not detected and repaired, a tile may detach on the next flight, resulting in severe damage to the vehicle structure. The ideal place to locate a thermal sensor is near the bottom of the gap, preferably in the filler bar strip that is placed down before tiles are installed. For a major Shuttle retrofit, sensors could be pre-installed every 5-10 cm inside the filler bar to monitor temperatures all over the vehicle. In any case, because exposure to a temperature above about 290°C will char the subsurface components, the sensor needs to indicate the occurrence of this temperature. Furthermore, to reliably record and report this over-temperature event, the device should be capable of withstanding short-term exposure to temperatures of 345°C or higher. In this application, the sensor must be replaced after the fuse is broken, but it should not need replacement before then. An over-temperature event will necessitate a TPS disassembly for subsurface inspection and repair, and a new sensor can be installed during the TPS reassembly.

If the sensor is to be inserted down into an existing gap, the constraints of the geometry suggest a "rice-grain" shape similar to the sensor shown in Figure 3. Figure 6 presents an image of an advanced prototype device. The main

components are a ferrite rod microantenna, two capacitors, a RFID microchip, and a thermal microfuse. As required, the components are bonded with electrically conductive epoxy or nonconductive epoxy. The components can survive long-term exposure to 315°C, except the microfuse opens at 292°C. The PROM microchip provides good thermal stability, but currently is not available with anticollision capability needed for long-term needs. (In the short term, an EEPROM anti-collision microchip could be used, but memory loss is possible with repeated exposure to high temperatures.) The lateral dimension of 0.12 cm allows insertion into larger inter-tile gaps for possible future flight testing on Shuttle.

Figure 7 is a sketch of the microfuse geometry. The microfuse design included selection of a fuse material, construction of a geometry that satisfies electrical, spatial, thermal, and mechanical constraints, and design of a housing to enclose both the microfuse and the flux needed to activate the solder. Eutectic solders, because of their precise melting points, are a good choice for use as the fuse material. The commercially available solder that best met our requirements was a Pb-Ag-Sn solder that melts at 292°C. The solder strip dimensions (50µm x 75µm x 400µm) are consistent with the width of the sensor and allow room for the cover. The strip resistance is much lower than 1 ohm and will not degrade the quality factor of the circuit. Order-of-magnitude calculations indicate there should be no serious mechanical difficulties from acceleration, vibration, or thermal expansion. Additionally, the thermal response of the fuse is much faster than alumina substrate, so thermal response of the sensor is dominated by conduction to the substrate. Heating tests confirm that the solder balls rapidly with short-term exposure above the melting point. The cover protects the fuse from damage, contains the flux needed to activate the solder, and prevents molten solder from shorting out the circuitry.

The tag circuit (Figure 8) uses two tuning capacitors. Initially the fuse is closed, and the resonant frequency of the device is determined by the parallel combination of the two capacitors, 103 kHz. If the fuse opens, the fuse capacitor is removed from the circuit, and the resonant frequency of the circuit increases to 156 kHz. This frequency separation is sufficient to provide discrimination between the two sensor states when the quality factor of the resonant circuit is sufficiently high. The tags were read using a modified version of the reader shown in Figure 3.

Although the bare tag can be handled with care (use of tweezers and gloves are recommended), we are considering use of a preceramic polymer coating to provide more durability and environmental protection. The tag can be dipped in the polymer solution, and used as is or cured in an oven at 130°C if required. The material is tougher and lighter in the cured state. The polymer is a hydrophobic, low-loss dielectric. A thin film with low mass provides waterproofing as well as protection from oils and salts.

To confirm the temperature capability and thermal performance of the advanced prototype, hot plate and oven tests were performed on tag components and on partially and fully-assembled tags. The tests showed that although the epoxy and polyimide components blackened at high temperature, the read range of the device after cooling was not affected by 15 minutes exposure to temperatures up to 350°C.

## PROTOTYPE ACTIVE SENSOR

An active wireless sensor uses battery power to assist in data acquisition and/or transmission. The basic idea is to measure and record the history of TPS parameters during flight. Figure 9 shows a cross-sectional view of the geometry. A RFID microchip circuit is placed in a relatively cool location at the bottom of a TPS tile (up to 125°C on Shuttle), and wires connect with various sensors located within the tile. Using wireless communications from an external reader, the user downloads to the device the criteria for data acquisition. The device proceeds to take and store data as instructed. At some later time, the user uploads the time-tagged data. The device acts as a self-contained experiment that may operate for one or more flights depending on the lifetime of the battery.

Figure 10 presents an image of the first prototype active tagged sensor that was assembled on circuit-board substrate. This sophisticated device contains several major components as follows:

**Battery.** A high-temperature-specification lithium battery with the highest capacity that fit the dimensional requirements was selected.

**Temperature signal conditioning.** A remote temperature is measured using a type-K thermocouple, whose output signal is applied to a precision analog signal-conditioning stage. The device temperature is measured using a

semiconductor temperature sensor located near the thermocouple reference junction. Both circuits output the temperature signal as a voltage to which a 10-bit analog-to-digital conversion is applied.

**Non-volatile memory.** Data are stored in a high-temperature-specification, EEPROM microchip to ensure data integrity. The memory also stores all related data, such as start time and sample period, required to reconstruct the temperature profiles.

**Real-time clock.** The clock uses a quartz crystal oscillator with high-temperature stability as its time reference.

**RFID transceiver.** The RFID transceiver circuit includes a demodulator to receive signals, a modulator to transmit signals, and the antenna coil. The circuit was designed to use the minimum number of components (to conserve area) while interfacing to the microcontroller and consuming the minimum amount of battery power. Battery power is not used for communication with the external reader. The ability to define and tune all circuit parameters enabled the transceiver to meet the requirements of transmission data rate and reading distance.

**Microcontroller.** The microcontroller configures the device for four modes of operation. *Power-down* mode is the default condition. The device is configured for minimum power and only listens for RFID communication. To enter this mode, the user can issue the stop command at any time. *Pre-datalog* mode is the wait period between mission start and data acquisition. Data acquisition may be initiated by time delay, device temperature, or thermocouple temperature. Therefore, the clock runs and the device periodically checks time or temperature as required to determine when to enter datalog mode. In *datalog* mode temperatures are sampled periodically per user-defined criteria. Data are processed and written to memory. When data acquisition is complete, the device enters post-datalog mode. *Post-datalog* mode is the same as power-down mode, except the clock continues to run until a user-issued stop command is received. This mode is limited to a two week period, because the clock is a continuous drain on the battery.

**Power supply.** A custom power supply was devised to meet the device lifetime requirement of 3 years and 45 use cycles. The battery voltage varies depending on temperature, usage, and other factors; however, some components such as the high-temperature memory and precision amplifiers, require up to 3.3 V. The solution was to use a regulator to supply a fixed voltage. However, even the most economical voltage regulator consumes enough power to flatten the battery within months. Therefore, a special power-supply topology was designed that features a low power mode, in addition to a 3.3 V supply mode. The microcontroller sets the mode according to the activity of the device. Because the microcontroller itself must be powered from the custom power supply, an added challenge was to ensure that the power was not interrupted when switching modes. The power-supply topology also allows the microcontroller to further reduce the power consumption by rationing power to individual circuit functions within the device. As shown in Table I, the average power consumption (which determines the overall drain on the battery) is relatively low. The device draws large peak currents when sampling the temperature or writing data to memory. The duration of the current surge is short at less than 4 ms. The largest power drain in non-power-down modes is the real-time clock.

**Reader and software** (not shown). Wireless communication is accomplished using an external reader and software on a laptop computer. The reader is a hand-held 17-cm square coil. The working range is about 15 cm, and the data transfer rate is about 3 kbit/s. Time and run parameters are downloaded to specific devices selected by tag ID number. At a later time, the tag ID number, digitized temperatures, and related data are uploaded using the reader. The software applies appropriate calibration functions to reconstruct the temperature profiles which are then displayed in graphical and tabular form. The calibration procedure is performed by the computer, rather than the microcontroller, in order to conserve battery power.

TABLE I. POWER USAGE OF ACTIVE TAGGED SENSOR.

Mode	Approximate Power [mW]	
	Average	Peak
Power-down	0.005	0.005
Pre-datalog	0.04	6 - 9 (depending on activation mode)
Datalog	0.04	11
Post-datalog	0.04	0.04

A test article was manufactured to demonstrate the capability and performance of the active tagged sensors. Two tags were installed at the back of a 21.5-cm square, 5-cm thick TPS tile. The thermocouples were placed at depths of 0.32 and 1.9 cm from the upper surface. The tile substrate is white, and a black (high emissivity) coating was applied to the upper and lateral surfaces.

The following experiment was performed. The sensors were programmed to take data for 512 seconds. After about 30 seconds a propane torch was applied to the center of the tile for one minute (Figure 11). At a later time, the sensor data were read by the external reader and plotted in Figure 12. The near-surface thermocouple measured over 600°C at the end of the heating period. The deeper thermocouple measured a heat conduction pulse beginning at 210 seconds (170 seconds after the start of heating) and is leveling off near 130°C at 500 seconds. The bottom of the tile remained at room temperature for the duration of the experiment.

## **FUTURE WORK**

The passive sensor design achieved the required RLV goals for mass, size, and temperature capability. Some mass reduction is possible by eliminating excess space on the substrate. A low-power, PROM-based 13.56 MHz chip with anti-collision architecture should be used when a suitable device becomes available. Operation at 13.56 MHz will allow faster communications, greater read range, and possible further size reduction to below 0.08 cm, if required, using a 0.05-cm dielectric rod in the core of the microantenna.

The main weakness of the design appears to be the performance of the microfuse and some epoxy bonds after cyclic heating. For the microfuse, more work is needed to insure that flux remains on the solder regardless of thermal cycling, vibrations, and accelerations that can occur on a RLV. The epoxy bond material decomposes at high temperature, and the device becomes susceptible to damage by vibration. Use of preceramic polymer for encapsulation to provide additional structural support may mitigate this problem. In any case, vacuum heating tests should be performed to ensure that the device remains operable and intact despite any outgassing and thermal decomposition that may occur.

A reliability goal of only one failure every 1-5 missions, with up to 25,000 tags on a vehicle, implies a 4-sigma to 6-sigma quality standard. Such reliability cannot be expected from hand-assembled prototypes, but may be possible in industrial mass production. With such a large number of tags, a few will experience data retention difficulties. In fact, exposure to radiation in the space environment is known to introduce single-event upsets [8]. Although the radiation dosage is fairly low in typical Shuttle orbits, these improbable random events do happen; however, the errors are most likely to occur in only one bit per tag. Error-correcting codes can be used to encode the ID number so that the tag will be immune to one (or more) bit upsets [9].

MEMS-based sensors would be ideal candidates for use in passive tags if they can meet size and temperature requirements. In particular, a MEMS device that could remember the highest temperature encountered, and then be reset by command from an external reader, could be used all over the vehicle to provide quantitative information on TPS performance and bond health.

The active sensor can be improved by incorporation of higher temperature components, higher frequency components, multiple sensors, and a custom microchip. An application-specific integrated circuit (ASIC) can be designed to reduce power consumption and area. Initial candidate circuit functions for replacement are the power supply and the RFID transceiver. Methods to reduce power consumption will be investigated, including in particular the real-time clock which is the largest single contributor. The battery is the main limitation of the active device. Active sensors cannot be widely used on a RLV until batteries of sufficiently small size, small mass, and long lifetime become available.

## **SUMMARY**

Issues and requirements for health monitoring of thermal protection systems on future reusable launch vehicles were discussed. Nondestructive evaluation technology is expected to make future inspection activities more automated, more reliable, and quicker than human-based inspection procedures currently being used on the Space Shuttle fleet. NASA Ames and industry partners are participating in a joint project to couple radio-frequency identification devices with event-recording sensors that can be embedded in and under the thermal protection system to monitor temperature or other quantities of interest. A passive prototype containing a thermal fuse to indicate a temperature overlimit, and an active prototype containing a thermocouple to measure a temperature history, were presented.

## ACKNOWLEDGEMENTS

This work was supported in part by contract NAS2-99092 to Eloret. The authors greatly appreciate the efforts of J.A. Marmie at NASA Ames, J.M. Heinemann at Eloret, D.G. Watters at SRI International, and K. Karunaratne at Korteks. The passive and active sensors were manufactured by SRI International and Korteks, respectively.

## REFERENCES

1. Anon., "Access to Space Study: Summary Report," Office of Space Systems Development, NASA Headquarters, NASA-TM-109693, Jan. 1994.
2. Anon., *Reusable Launch Vehicle: Technology Development and Test Program*, National Research Council Committee on Reusable Launch Vehicle Technology and Test Program, National Academy Press, Washington, DC, 1995.
3. Gordon, M.P., "Investigation of Shuttle Thermal Protection System Health Monitoring," Boeing Reusable Space Systems, Orbiter Engineering Report KLO-99-003, Kennedy Space Center, FL, Sept. 1995.
4. Pallix, J.B., Milos, F.S., and Huestis, D.L., "Subsurface Microsensors for Assisted Recertification of TPS (SmarTPS)," *ICCE/6 Sixth Annual International Conference on Composites Engineering*, edited by D. Hui, ICCE and College of Engineering, University of New Orleans, June 1999, pp. 635-636.
5. Milos, F.S., Watters, D.G., Pallix, J.B., Bahr, A.J., and Huestis, D.L., July 2001. "Wireless Subsurface Microsensors for Health Monitoring of Thermal Protection Systems on Hypersonic Vehicles," in *Advanced Nondestructive Evaluation Methods and Applications*, edited by T. Kundu, Proceedings of SPIE, Vol. 4335, pp. 74-82, 2001.
6. Watters, D.G., Bahr, A.J., and Huestis, D.L., "High-Temperature SensorTags for Health Monitoring of Thermal Protection Systems: An Update on Wireless Microsensor Development for SmarTPS," SRI Final Report, Project 10731, Menlo Park, CA, Dec. 2000.
7. Karunaratne, K., "Smart TMS Phase II User Guide," Korteks, San Diego, CA, Jan. 2001.
8. Messinger, G.C., and Ash, M.S., *Single Event Phenomena*, Chapman and Hall, 1997.
9. Gray, K., "Adding Error-Correcting Circuitry to ASIC Memory," *IEEE Spectrum*, Vol. 37, No. 4, 2000, pp. 55-60.

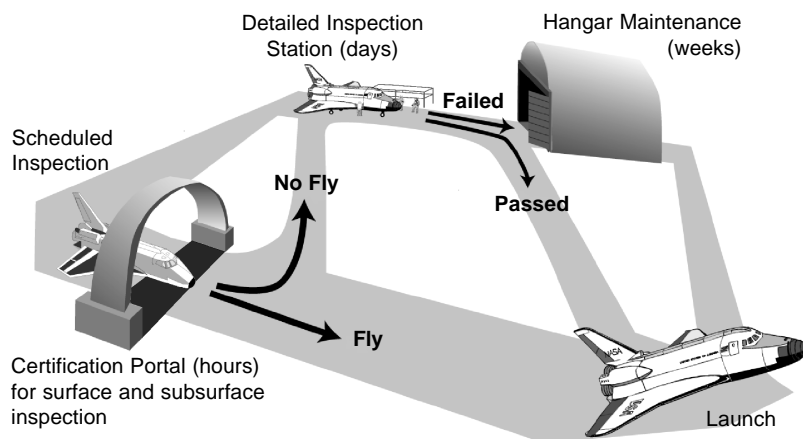
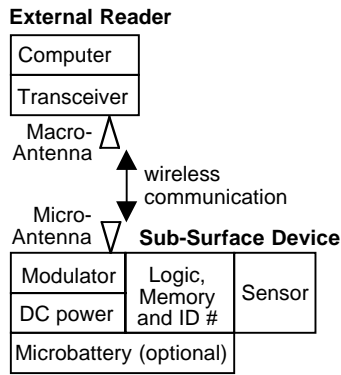
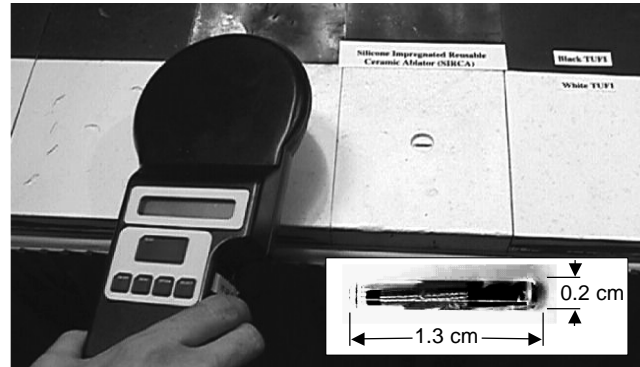


Figure 1. Futuristic TPS inspection process.



**Figure 2.** System block diagram for RFID-tagged sensor.



**Figure 3.** Demonstration of communication through various TPS materials to RFID tags (insert) at 125 kHz.



**Figure 4.** Demonstration of rapid communication with many RFID tags at 125 kHz using anti-collision technology.

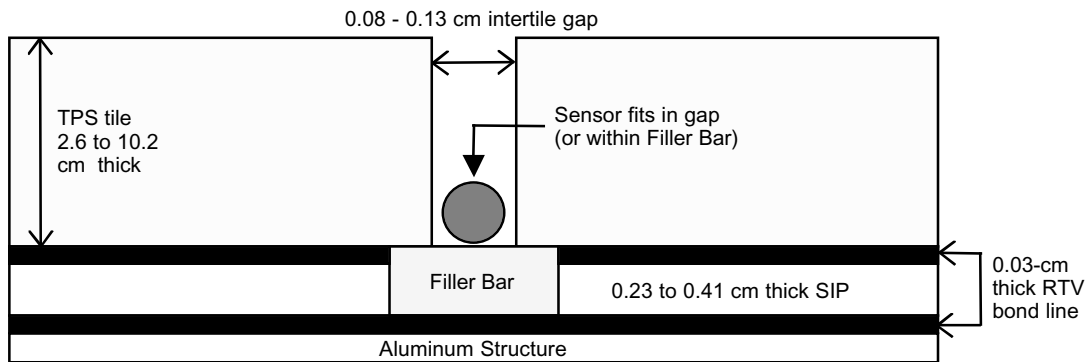


**Figure 5.** Cross-section of Shuttle TPS stackup showing placement of thermal sensor.



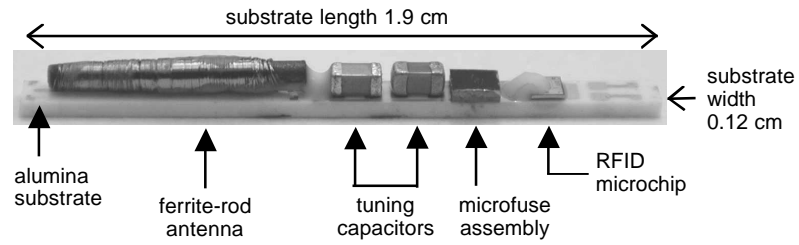


**Figure 6.** Advanced prototype passive tagged sensor, 80 mg.

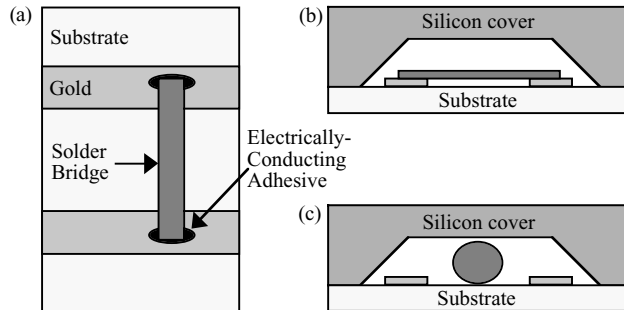


**Figure 7.** Thin-film microfuse design: (a) top view of uncovered microfuse on alumina substrate, (b) side view of covered microfuse (closed circuit), (c) side view of covered microfuse (open circuit). The cover provides sufficient space for the solder to bead upon melting, thereby opening the circuit.

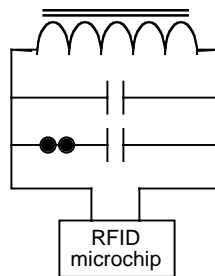
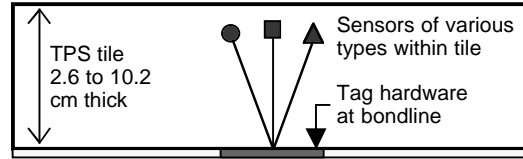


**Figure 8.** Circuit diagram for passive tagged sensor.

Front Surface: temperature can exceed 1200°C in flight.



Back Surface: temperature up to 125°C on Shuttle.  
May need to survive up to 350°C in future applications.

**Figure 9.** Installation diagram for active tagged sensor.

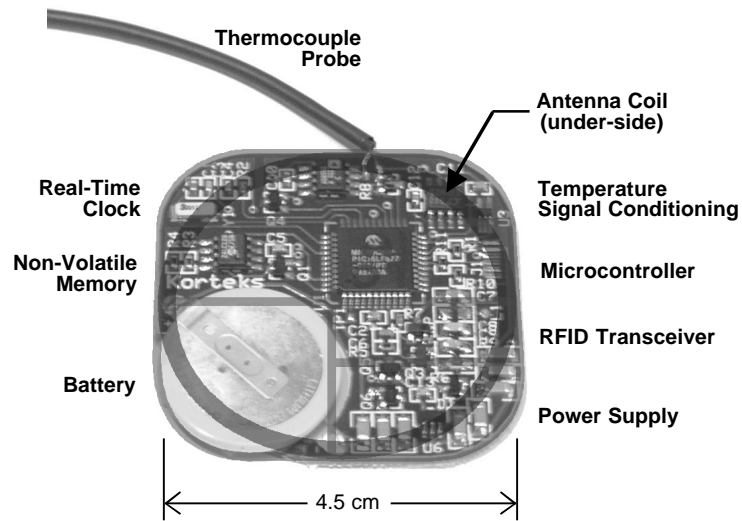


**Figure 10.** Components of active tagged sensor.

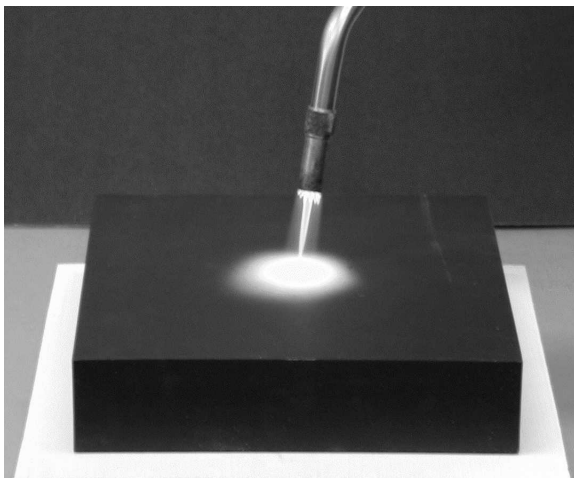


**Figure 11.** Propane torch applied to TPS tile containing two active sensors.

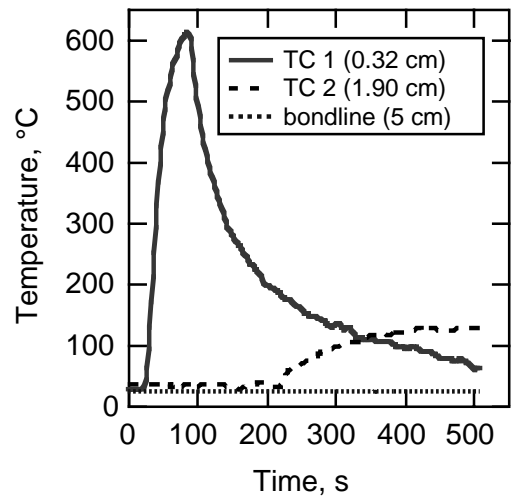


**Figure 12.** Data from blowtorch experiment.